Migration without interbreeding: evolutionary history of a highly selfing Mediterranean grass inferred from whole genomes

Christoph Stritt[1,2], Elena L. Gimmi[1,3], Michele Wyler[1], Abdelmonaim H. Bakali[4], Aleksandra Skalska[5], Robert Hasterok[5], Luis A. J. Mur[6], Nicola Pecchioni[7], Anne C. Roulin[1*]

[1] Institute for Plant and Microbial Biology, University of Zurich, Zurich, Switzerland; [2] Current address: Department of Medical Parasitology and Infection Biology, Swiss Tropical and Public Health Institute, Basel, Switzerland; [3] Current address: Department Aquatic Ecology, Swiss Federal Institute of Aquatic Science and Technology Eawag, Dubendorf, Switzerland; [4] National Institute of Agronomy, Regional Center of Errachidia, Errachidia, Morocco; [5] Institute of Biology, Biotechnology and Environmental Protection, Faculty of Natural Sciences, University of Silesia in Katowice, Katowice, Poland; [6] Institute of Biological, Environmental and Rural Sciences, Aberystwyth University, Wales, UK; [7] Research Centre for Cereal and Industrial Crops, CREA – Council for Agricultural Research and Economics, Foggia, Italy

Corresponding author: anne.roulin@botinst.uzh.ch

ABSTRACT

Wild plant populations show extensive genetic subdivision and are far from the ideal of panmixia which permeates population genetic theory. Understanding the spatial and temporal scale of population structure is therefore fundamental for empirical population genetics – and of interest in itself, as it yields insights into the history and biology of a species. In this study we extend the genomic resources for the wild Mediterranean grass *Brachypodium distachyon* to investigate the scale of population structure and its underlying history at whole-genome resolution. 86 accessions were sampled at local and regional scales in Italy and France, which closes a conspicuous gap in the collection for this model organism. The analysis of 196 accessions, spanning the Mediterranean from Spain to Iraq, suggests that the interplay of high selfing and seed dispersal rates has shaped genetic structure in *B. distachyon*. At the continental scale, the evolution in *B. distachyon* is characterized by the independent expansion of three lineages during the Upper Pleistocene. Today, these lineages may occur on the same meadow yet do not interbreed. At the regional scale, dispersal and selfing interact and maintain high genotypic diversity, thus challenging the textbook notion that selfing in finite populations implies reduced diversity. Our study extends the population genomic resources for *B. distachyon* and suggests that an important use of this wild plant model is to investigate how selfing and dispersal, two processes typically studied separately, interact in colonizing plant species.

Keywords: population structure, selfing, seed dispersal, heterozygosity, range expansion, flowering time

Introduction

In population genetic theory, a population is a matter of definition. In the natural world, populations are part of complex geographic mosaics; they can be discrete, continuous, or somewhere in-between; and they can expand and contract, appear and disappear. In short, answering the question "What is a population?" is not straightforward for most species (Waples & Gaggiotti, 2006). Yet answering it, implicitly or explicitly, establishes the link between theory and data and is the first step for many studies in ecology, evolution, and conservation.

The concept of population structure or subdivision subsumes many of the challenges of empirical population genetics (Wright, 1931; Hey & Machado, 2003). Population structure results from the phylogeographic and demographic history of the species (Nieto Feliner, 2014; Charlesworth, 2009), life history traits such as dispersal mode and breeding system (Loveless & Hamrick, 1984), and ecological interactions and adaptation (Linhart & Grant, 1996). Disentangling how these different processes contribute to genetic diversity and differentiation is a major goal of evolutionary biology. As processes are inferred from patterns, for any species the disentangling ideally begins with a thorough analysis of population subdivision, that is, of the spatial and temporal scale of genetic differentiation (e.g. Platt et al., 2010).

In the past years, the resolution at which population structure can be analysed has increased greatly due to the availability of genomic data (Pannell & Fields, 2014). Sampling genealogies along genomes allows to overcome problems due to the high stochasticity of single gene trees (Hey & Machado, 2003). Furthermore, measures of absolute genetic divergence such as d_{XY} can replace or complement more assumption-rich statistics such as F_{ST}, which rely on *a priori* definitions of popula-

tions and can be confounded by within-population structure or the sampling of close relatives (Putman & Carbone, 2014).

In this study we investigate the scale of population structure in the Mediterranean grass *Brachypodium distachyon* and infer its underlying history of population divergence. *B. distachyon* naturally occurs around the Mediterranean Basin and is a specialist of arid, oligotrophic habitats characterized by recurrent disturbance (San Miguel, 2008; López-Alvarez et al., 2015). It has a fully assembled diploid 272 Mb genome (International Brachypodium Initiative, 2010) and is an established model to study various aspects of grass biology (Vogel, 2016, Scholthof et al., 2018). Its value as a model for plant evolution lies in its Mediterranean distribution, providing a window into an ecologically precious yet understudied region (Thompson, 2005); its belonging to the Poaceae, a plant family dominating terrestrial ecosystems around the globe (Gibson, 2009); and, finally, its genome of intermediate complexity, where numerous gene copy number variants (Gordon et al., 2017) and transposable element polymorphisms (Stritt et al., 2018, 2020) contribute to molecular evolution.

A key question which has emerged from previous population genetic studies with *B. distachyon* concerns the role of seed dispersal in shaping genetic structure. A large-scale microsatellite survey in Turkey reported high genotypic diversity within and little differentiation between populations (Vogel et al., 2009). This was explained through a combination of long-distance seed dispersal and extreme selfing rates, the former shuffling genotypes across the landscape, the latter preventing gene flow between diverged genotypes. Other studies, however, found little diversity within and high differentiation between populations in Turkey (Dell'Acqua et al., 2014) and Spain (Marques et al., 2017), in agreement with the increased genetic drift expected in selfing organisms (Charlesworth, 2003). How-

ever, as these studies considered different populations and used different sampling schemes, it remains difficult to tell whether their disagreement reflects different biological realities or study designs.

A second pattern highlighted by previous studies is the sympatry of highly diverged lineages differing in flowering phenology (Tyler et al., 2016; Gordon et al., 2017; Sancho et al., 2018). As in other widespread annual plants (e.g. Engelmann & Purugganan, 2006), genetic variation for the control of flowering is present in *B. distachyon*, in particular in the vernalization pathway preventing the development of flowers in the cold season (Ream et al., 2014). It has been suggested that differences in flowering phenology could explain the lack of admixture between sympatric lineages (Gordon et al., 2017). This hypothesis, however, is difficult to evaluate as long as the role of phenotypic plasticity in flowering and the biogeographic history underlying the large-scale distribution of lineages remain unknown.

Here we extend the genomic resources for *B. distachyon* with whole-genome sequences for 75 Italian and 11 French accessions sampled at local and regional scales. Besides filling a conspicuous geographical gap in the *B. distachyon* collection, our aim was to sample across different spatial scales in order to better understand the scale of population structure in this species. Combining these resources with publicly available data, we describe the scale of population structure in 196 accessions spanning the Mediterranean from Spain to Iraq, infer the underlying history of population divergence, and discuss how the interplay of selfing and dispersal has shaped genetic structure across spatial and temporal scales. Furthermore, we conducted flowering time experiments illustrating the phenotypic plasticity of flowering phenology and suggesting caution when extrapolating from greenhouse experiments to natural populations.

Material & Methods

Sampling & Sequencing

719 dry *Brachypodium* plants were collected in 2016 across Italy, in the Languedoc region in Southern France, and in 2018 across the Atlas Mountains of Morocco (Table S1). A representative set of 276 accessions were grown in the greenhouse from single seeds. Their DNA was extracted from leaves with a CTAB-based method (Stein et al., 2001), quality-checked with Nanodrop (NanoDrop Technologies Inc), and quantified with Qubit (Invitrogen).

As *B. distachyon* may be confounded with its morphologically similar sister species *B. stacei* and *B. hybridum* (Catalan et al., 2016), we first identified the species of the 276 accessions using the microsatellite marker ALB165 (Giraldo et al., 2012) and by sequencing the GIGANTEA gene (López-Alvarez et al., 2012) with ABI SOLiD. 143 individuals were identified as *B. distachyon*, 130 as *B. hybridum*, and three as *B. stacei* (Table S1). All 70 accessions collected in Morocco proved to be *B. hybridum* and were not included in this study.

86 out of the 143 genotyped *B. distachyon* accessions were selected for sequencing. In order to reduce the chance of sequencing close relatives, only accessions collected at least 50 meters apart were included. In addition, we also sequenced the reference accession Bd21 as a control and the *B. stacei* accession Cef2 as an outgroup for phylogenetic analyses. Paired-end libraries were prepared with the PCR-free KAPA Hyper Prep Kit (KAPA Biosystems). The 150 bp paired-end reads were sequenced with Illumina HiSeq2500 at the Genomics Facility Basel to a mean coverage of 23 (range 18–38, Table S1). The resulting sequencing data were joined with 57 recently sequenced Turkish accessions (Skalska et al., 2020; mean coverage 36) and with data for 52 accessions originating mainly from Spain and Tur-

key (Gordon et al., 2017). To speed up computation and avoid bias due to unequal coverage, the latter reads were downsampled to a mean coverage of 30 using Picard tools v.1.97 (broadinstitute.github.io/picard). The total number of accessions analysed in this study is thus 86 + Bd21 + 57 + 52 = 196.

Alignment, variant calling & filtering

Paired-end reads were aligned to version 3.0 of the *B. distachyon* Bd21 reference genome, downloaded from Phytozome 12, with BWA MEM v. 0.7.12-r1039 (Li, 2013). Aligned reads were converted to the bam format and sorted with samtools v. 1.9 (Li et al., 2009), and read duplicates were removed with sambamba (Tarasov et al., 2015). Variants were then called with GATK v. 4.0.2.1. The following hard-filtering thresholds were applied to the combined variants: only SNPs were retained with a quality-by-depth > 20, a Phred score < 20 for Fisher's exact test for strand bias, and a *Z*-score between -1 and 1 for Wilcoxon's rank sum test of Alt vs. Ref read mapping qualities. Additionally we removed SNPs in low complexity regions identified with dustmasker (Morgulis et al., 2006), resulting in a total of 8,426,015 hard-filtered SNPs.

Dealing with artificial heterozygosity due to structural variants

Identifying heterozygous SNPs in *B. distachyon* is complicated by a high number of gene copy number variants (Gordon et al., 2017). If a stretch of DNA is duplicated in a sequenced accession but present as a single copy in the reference, sequencing reads derived from the duplicates are collapsed onto a single region when aligning them to the reference genome. Depending on the divergence of the duplicates, this may give rise to islands of extended heterozygosity (IEH): regions of up to few thousand base pairs with extreme numbers of heterozygous sites (Figure S1). As wrongly identified heterozygosity might severely bias downstream analyses, in particular the estimation of selfing rates, we first quantified the issue by scanning each accession for IEH. An IEH was recorded if there were ten or more heterozygous

126 SNPs along a distance of at least 300 bp. The program implementing this approach (detectIEH.py) is
127 available on github.com/cstritt/popgen.

128 Because hard filtering proved insufficient to deal with the artificial heterozygosity identified
129 in the previous step, we used a masking approach to obtain high-confidence SNPs, including hetero-
130 zygous sites. For each accession a mask was created indicating the regions in the genome within 1.5
131 standard deviations of the accession-specific mean read coverage. In this way, an average of 85% of the
132 genome was included per accession (range 76% [Bd1-1] to 88% [Bd21]). In a next step, the individual
133 masks were combined with bedtools (Quinlan & Hall, 2010) to define high-confidence regions as re-
134 gions with "normal" coverage in at least 90 percent of the accessions. Removing SNPs outside these re-
135 gions resulted in a set of 5,774,928 SNPs across the 196 accessions. These variants are referred to as
136 high-confidence SNPs in the following.

137 Population structure and historical gene flow

138 Genetic structure was analysed using principal component analysis and ancestry coefficient estimation.
139 For the principal component analysis, the 5,774,928 SNPs in high-confidence regions were used and
140 additionally filtered with the snpgdsLDpruning function of the R package SNPrelate (Zheng et al.,
141 2012). Only SNPs were retained with a minor allele frequency > 0.05 and a composite linkage disequi-
142 librium < 0.4, resulting in 14,485 informative SNPs. The snpgdsPCA function of the same package was
143 used to calculate the components. Ancestry coefficients were estimated with sNMF, as implemented in
144 the R package LEA (Frichot & François, 2015), a method appropriate for high levels of inbreeding as it
145 does not assume Hardy-Weinberg equilibrium. Using the same SNPs as for the PCA, sNMF was run
146 for K values from 2 to 20, with 10 repetitions per K.

147 A rooted phylogeny was estimated with SNPhylo (Lee et al., 2014). For this analysis we selec-
148 ted synonymous sites in the high-confidence SNP set and additionally filtered them for a minor allele
149 frequency of 0.05, a maximum missing rate of 0.1, and a maximum linkage disequilibrium (r^2) of 0.4,
150 resulting in 5,432 LD-pruned synonymous sites. The root was set to the *B. stacei* accession Cef2, se-
151 quenced for this study. 100 bootstrap replicates were performed to assess the robustness of the tree.

152 fineSTRUCTURE v. 4.0.1 (Lawson et al., 2012) was used to obtain a more detailed picture of
153 population subdivision in *B. distachyon*. This method leverages haplotype information to infer shared
154 ancestry between individuals. More specifically, it estimates the number and lengths of chunks along
155 the genome of individual *i* coalescing with individual *j* before they coalesce with any other individual.
156 The program output we present is a similarity matrix which indicates the recombination map distance a
157 "recipient" genotype (rows) receives from the "donor" genotypes (columns). As fineSTRUCTURE
158 models linkage disequilibrium and performs best with dense haplotype data, the 8,426,015 hard-filtered
159 SNPs were used after removing heterozygous sites and missing data, resulting in 3,467,964 SNPs. By
160 removing heterozygous sites the accessions are treated as haploid and no phasing is thus required. Re-
161 combination distances between loci were obtained from the linkage map of Huo et al. (2011). fineS-
162 TRUCTURE was run in its haploid mode, using default settings.

163 To test whether shared ancestry is better explained by common descent or historical gene flow,
164 TreeMix (Pickrell & Pritchard, 2012) was used to model migration. The high-confidence SNP set was
165 used, with 4,473,162 variable sites after removing missing data. To account for linkage disequilibrium,
166 a block size k of 2,000 SNPs was defined, which corresponds to an average distance of 120 kb in the
167 genome. Models with zero to four migration edges *m* were tested, with 100 independent runs for each
168 *m*. For each model, the run achieving the highest likelihoods was used for model comparison.

Linkage disequilibrium

Selfing has important consequences for the extent of linkage disequilibrium (LD). The effective recombination rate is $1 - s$ times slower with selfing because meiotic recombination is mainly reshuffling homozygous alleles (Nordborg 2000), resulting in extensive linkage disequilibrium. On the other hand, population substructure in the absence of gene flow decreases LD as mutations accumulate in independently evolving lineages (Hartfield et al., 2018). We estimated linkage disequilibrium at different scales of population structure with PopLDdecay (Zhang et al. 2019). LD is reported as r^2 averaged over pairwise comparisons. The high-confidence SNP set was used with default program settings (-MAF 0.05, -Miss 0.25). To assess the effect of population subdivision on LD, we used the sum of terminal branch lengths in subtrees as a measure of how much independent evolution has occurred in different subtrees.

Estimation of divergence times

To put a timescale on the divergence in *B. distachyon*, we used the multispecies coalescent approach implemented in BPP v.4.2.9 (Rannala & Yang, 2003; Flouri et al., 2018). 20 diverse accessions were selected to represent the *B. distachyon* phylogeny. 200 random genomic regions of 1 kb length and at least 100 kb apart were chosen, as BPP assumes no recombination within and free recombination between loci. For each of the 20 accessions the 200 sequences were obtained by calling consensus sequences from the respective bam file. Potential problems of paralogy were avoided by considering only reads with a mapping quality > 30, which excludes reads mapping to multiple places in the genome. Inverse gamma priors were set to (3, 0.014) for the root age τ and to (3, 0.002) for the population size parameter θ, which corresponds to a mean theta of 0.001 and a mean root age of one million years, assuming a constant mutation rate of 7×10^{-9} substitutions per site per generation (Ossowski et al. 2010).

191 The rooted species tree was defined as (((A_East, A_Italia), (B_East, B_West)), C_Italia), as inferred
192 with the SNPhylo analysis described above. The MCMC was run four times independently, each time
193 with 408,000 iterations, including a burn-in of 8000 iterations and samples taken every second itera-
194 tion. Convergence of the four runs was assessed with Tracer (Rambaut et al., 2018).

195 Genetic diversity and population differentiation

196 To estimate genetic diversity and differentiation, we estimated absolute genetic differentiation d_{XY} at
197 synonymous sites. The --includeNonVariantSites option of GATK v.3.4 was used to obtain variable and
198 non-variable synonymous sites. For each pairwise comparison between the 196 accessions, we then
199 calculated the number of variable and the total number of sites. Heterozygous sites were ignored and
200 only sites were considered for which both accessions in the comparison had a read coverage within 1.5
201 standard deviations of the accession-specific mean coverage. The script implementing this procedure
202 (pairwise_nucdiff.py) is provided on github.com/cstritt/popgen. Pairwise geographic distances were
203 calculated as Great Circle (WGS84 ellipsoid) distances between each pair, using the spDistsN1 func-
204 tion of the R package sp (Pebesma & Bivand, 2005). Mantel tests were used to test for isolation by dis-
205 tance, using the mantel.rtest function of the ade4 package with 100 permutations to assess the signific-
206 ance of the correlations (Dray & Dufour, 2007). To test if genetic diversity differs between regions, a
207 Kruskal-Wallis test was performed followed by Dunn's test for multiple comparisons with a Benjamini-
208 Hochberg correction.

209 Flowering time experiments

210 Two experiments were conducted to investigate how flowering phenology relates to genetic structure in
211 *B. distachyon.* Firstly, we tested how the newly sampled accessions respond to vernalization treatments
212 ranging from 0 to 12 weeks at 4°C under short-day conditions in the greenhouse. Twelve Italian acces-

213 sions with different geographic origins were analysed (Cro24, Cm2, Leo2, Mca23, Mca18, Msa27,
214 Ren22, San12, Sap49, Spm16, Sul5, Tar1). We further used four control accessions from Turkey and
215 Iraq (Bd1-1, Bd3-1, BdTR3C, BdTR7a) previously investigated (Ream et al., 2014; Sharma et al.,
216 2017) in order to confirm the reproducibility of the flowering behaviour and vernalization require-
217 ments. Plants from all 16 accessions were germinated for three weeks in the greenhouse. They were
218 subsequently put in a cooling chamber for 0, 4, 6, 8, 10 or 12 weeks, respectively, and transferred to the
219 greenhouse again. Three to five replicates were used per accession per time point. Time until flowering
220 was counted from the day after the return to warm conditions (directly after the first three weeks of ger-
221 mination for the plants with 0 weeks vernalization). Flowering was defined as the emergence of the
222 first spike. The cooling chamber was set to 4°C, 8 h light and 16 h dark. The greenhouse conditions
223 were 16 h day at 20–21°C and 8 h dark at 18°C with a light intensity of 200 umol PAR and 60% relat-
224 ive humidity over the entire experiment.

225 In the wild, plants all go through a prolonged vernalization process during winter which might
226 produce different outcomes than the conditions tested in the greenhouse. To test for this possibility, we
227 planted seeds of 105 accessions outdoors in November 2017, in the Botanical Garden of Zurich,
228 Switzerland, with six replicates per accession. Only six plants did not germinate and 624 plants were
229 used for phenotyping. To ensure no bias due to position effect, replicates were distributed randomly
230 across trays. Mild heating was applied at the bottom of the compartment to prevent freezing when out-
231 door temperature fell below –10° C. From April 2018 on, plants were checked every three to four days
232 for flowering. The first plant flowered the 21st of April 2018, which was used as a reference (day 1).
233 About 14% of the replicates from the A lineage desiccated before the end of the experiment and did not
234 reach flowering. To test for differences in flowering time between clades a linear mixed effects model

was used, as implemented in the R package MCMCglmm (Hadfield, 2010). To control for the six biological replicates, individual accessions were treated as random effects in the model.

Results

Occurrence of *Brachypodium distachyon*

B. distachyon, *B. stacei*, and their allotetraploid hybrid *B. hybridum* are now known to be different species (Catalán et al., 2012), while they were considered different cytotypes of *B. distachyon* until 2012. As botanical collections do not distinguish between the three species, their relative distribution around the Mediterranean and beyond is still vague. We found that, in agreement with general habitat descriptions (Catalán et al., 2016), *B. hybridum* was more frequent in the drier South of Italy, while *B. distachyon* was predominant in Northern Italy and France (Table S1). Only three plants were genotyped as *B. stacei*, in agreement with this species being the rarest of the three (Table S1). Furthermore, we found only *B. hybridum* in Morocco, suggesting that *B. distachyon* might be rare on the African continent.

Single nucleotide polymorphisms: beware of artificial heterozygosity

As mentioned above, a significant proportion of the initial 8,426,015 hard-filtered SNPs were observed to aggregate in islands of extended heterozygosity (IEH, Figure S1). IEH can be artefacts which arise when reads from paralogous stretches of DNA are collapsed onto a single region in the reference genome; but they can also represent real heterozygosity in the case of recent admixture between diverged lineages. To distinguish the two possibilities, we compared IEH among the initial hard-filtered SNPs and 5,774,928 SNPs in high-confidence regions, defined as regions where at least 90 percent of the accessions have a read coverage within 1.5 standard deviations of their mean coverage. If a region has a

255 coverage within this "normal" range, this indicates that it was not deleted or duplicated in the se-
256 quenced accession, and that heterozygous sites are thus not due to collapsed paralogs.

257 A median of 116 IEH were identified per accession in the hard-filtered set as compared to only
258 two in the high-confidence set (Figure 1), indicating that most IEH are artefacts caused by structural
259 variants. Six accessions (Uni2, Mig3, ABR9, Bd21-3, ABR7, Per1) deviate from the general pattern
260 and have hundreds of IEH even in high confidence regions (Figure 1a). As the sequencing depth at
261 these IEH is within the normal range and does not suggest the presence of structural variation (Figure
262 S2), we propose that this is real heterozygosity left over from recent interbreeding between diverged
263 genotypes. On average 46% of the IEH identified in any accession overlap with annotated genes, with a
264 median of 50 genes per accession showing evidence of extended heterozygosity. As expected from the
265 composition of the pan-genome (Gordon et al., 2017), the total set of 4,211 genes with IEH is enriched
266 for the GO terms "defence response", "response to stress" and other functions associated with highly
267 dynamic gene families.

268 Three major lineage and five large geographic clades of *B. distachyon*

269 The different clustering methods capture a clear subdivision of the 196 accessions into five major ge-
270 netic clades, except for two accessions from the Pyrenees which cannot be assigned (Arn1 and Mon3;
271 Figure 2a). This subdivision is particularly clear in the sNMF analysis, where model fit improves in
272 large steps until K=5, after which it declines in smaller steps as regional and local populations are re-
273 covered (Figure 2b), as also shown in an Evanno-like evaluation of the "best" K (Figure S3; Evanno et
274 al., 2005). At the base of the rooted *B. distachyon* phylogeny (Figure 2c,e; Figure S4; an interactive
275 tree/map is provided on github.com/cstritt/bdis-phylogeo), 15 Italian accessions form a clade (hereafter
276 called C_Italia) consisting of nine plants from the Gargano peninsula in south-eastern Italy and six col-

lected across Italy, namely in Sicily, southern Campania and Liguria (Figure 2a). After the divergence of this basal lineage, the tree splits into two large lineages: one comprising all the remaining plants from Italy (A_Italia) and plants primarily from the coastal regions of Turkey (A_East), the other comprising plants from the western Mediterranean (B_West) and plants primarily from the Anatolian plateau and south-eastern Turkey/Iraq (B_East). The same subdivision is evident in the PCA (Figure 2d). A geographic outlier are three accessions from southern Turkey (2_20_16, 2_14_15 and 2_14_20; Figure 2a) which cluster with accessions from Spain and France. As these Turkish accessions were collected recently (Skalska et al., 2020) and not grown in contact with Spanish or French accessions, this finding can hardly be explained by mislabelling or seed contamination.

Using the multispecies coalescent approach implemented in BPP (Figure 2c), the split between the basal C lineage and the others is dated to 107 thousand years ago (kya, 95% highest posterior density interval [HPDI] 86–128 ky) and the split between the A and B lineages to 52 kya (95% HPDI 35–72 ky). Within the A lineage, the separation between A_East and A_Italia is dated to 18 kya (95% HPDI 8–27 ky), while within the B lineage the separation between B_East and B_West is estimated at 22 kya (95% HPDI 15–30 ky).

Little evidence for historical gene flow between diverged lineages

At this coarse level of genetic structure, we thus observe an incongruence between genetic structure and geographic occurrence. Roughly half of the plants collected in Turkey and Iraq are more closely related to plants from the western Mediterranean than to other plants from the east. Similarly, in Italy the majority of the collected plants are more closely related to plants from the east than to the 15 Italian plants at the base of the phylogeny. In the east, the A and the B lineage might occur in the same locality, yet there is a clear overall geographic division (Figure 2a; github.com/cstritt/bdis-phylogeo; see also

299 Skalska et al., 2020): lineage A is predominant in the coastal region, lineage B on the inland Anatolian
300 plateau and in the Fertile Crescent. In Italy the occurrence of the A and the C lineage is less clear-cut: in
301 two of the four localities where lineage C was found, plants of the A and the C lineage were present on
302 the same meadow and thus sympatric in a narrow sense (Figure S5).

303 Estimates of shared ancestry show little evidence for recent gene flow between co-occurring
304 lineages in Turkey and Italy (Figure 2a,e). Historical gene flow between geographic clades appears pos-
305 sible, yet the evidence is not particularly strong: a tree-like model without migration edges explains
306 99.7% of the covariance of allele frequencies between geographic clades (Figure S6), suggesting that
307 shared ancestry apparent in Figure 2 is due to common descent and shared genetic drift rather than ad-
308 mixture. Adding a migration edge leading from A_East to B_East leads to an increase to 99.98%, sug-
309 gesting that, if historical gene flow has occurred, it has not left strong signatures.

310 High selfing rates and a strong effect of subdivision on linkage disequilibrium

311 Selfing rates often vary within species (Barrett, 2003; Griffin & Willi, 2014), yet studies with *B. dista-*
312 *chyon* have all reported a near absence of heterozygosity (Vogel et al., 2009; Marques et al., 2017). To
313 test whether this pattern holds across geographic regions, we estimated inbreeding coefficients and self-
314 ing rates for the 196 accessions. Using SNPs in high-confidence regions, as defined above, we estim-
315 ated a median inbreeding coefficient F of 0.996 among the 196 accessions (mad=0.003, Table S1),
316 which translates to a median selfing rate of 0.998 using s = 2F / 1+F. When population structure is
317 taken into account and F is estimated within geographic clades, median F is 0.991 and thus only mar-
318 ginally lower than at the species level. As expected, lower F values are estimated for the six accessions
319 whose genomes contain numerous IEH. Overall, our results show that extreme levels of homozygosity

320 and high selfing rates predominate throughout the species' range and vary little between subpopula-
321 tions.

322 LD is low at the species level (Figure 3a) and successively increases as one considers finer
323 scales of subdivision (Figure 3b-d). A comparison of LD decay and the topology of the *B. distachyon*
324 phylogeny supports the expectation that LD decay reflects substructure rather than recombination. Us-
325 ing the sum of terminal branch lengths in subtrees as a measure of how much independent accumula-
326 tion of mutations has occurred at different levels, we observe a strong negative relation between mean
327 r^2 at a distance of 100 kb and the sum of terminal branch lengths (Figure S7): LD decay is slower in
328 subtrees containing either few leaves, e.g. in the C lineage, or containing short terminal branches, as in
329 B_East, where there is a surprising number of genetically highly similar accessions.

330 Strong isolation by distance within the three major lineages

331 To understand how genetic diversity is partitioned across space and the different levels of genetic struc-
332 ture in *B. distachyon*, we estimated pairwise genetic differences (d_{XY}) at synonymous sites. Within the
333 five geographic clades, median d_{XY} is 0.0018, that is, 1.8 different sites per 1000 bp (Figure 4a). Values
334 differ somewhat among clades: d_{XY} is higher in A_East (0.0019) than in the other lineages ($P<2x10^{-16}$,
335 Kruskal-Wallis), and lower in C_Italia (0.0017) than in the others ($P<0.03$). Levels of diversity in the
336 B_East and B_West clades are similar (0.0017, $P=0.37$). Between clades, d_{XY} reaches up to 0.0065 in
337 comparisons between C_Italia and B_West.

338 Within all three major lineages, d_{XY} increases with geographic distance, as shown by signific-
339 ant Mantel correlations (Figure 4b). While correlation coefficients are similar between lineages
340 ($r_A=0.75$, $r_B=0.71$, $r_C=0.77$), some deviations are observed in the B lineage. On the one hand, there are
341 genetically similar accessions with distant geographic origins, particularly in the B_East clade, in

342 agreement with the previously observed poor mapping between geography and phylogeny in this clade.
343 On the other hand, genetically distant individuals can be geographically close (upper left of the middle
344 panel in Figure 4b). These are comparisons of Turkish accessions with the three accessions collected in
345 Turkey clustering genetically with B_West accessions (Figure 2a).

346 The hierarchical nature of population subdivision

347 Population subdivision in *B. distachyon* is hierarchical and does not end at level of the five geographic
348 clades. Substructure is evident for increasing values of K in the sNMF analysis (Figure S8), in within-
349 lineage PCAs (Figure S9), as subtrees in the phylogeny (Figure S4), and most clearly in the fineS-
350 TRUCTURE analysis (Figure 2e). The clustering algorithm implemented in fineSTRUCTURE identi-
351 fies 59 populations with a median size of two (range 1-13). This inflated number of populations most
352 likely reflects the limitations of formal approaches to identify the "most realistic" number of popula-
353 tions in a highly selfing organism, where the homogenizing force of gene flow is limited and popula-
354 tions are better understood as phylogenetic clades than as panmictic units.

355 In *B. distachyon,* many subtrees cluster geographically into regional populations (Figure 2e;
356 github.com/cstritt/bdis-phylogeo). In the A_Italia clade, populations from Campania, Abruzzo and Gar-
357 gano in the South and from Toscana and Emilia-Romagna in the North can be distinguished. Also in the
358 other lineage present in Italy, C_Italia, the 15 samples cluster according to their geographic origin. In
359 the western Mediterranean, the Pyrenees separate a Spanish from a French population comprising all
360 the newly collected accessions from the Languedoc region. Substructure is less obvious in the east.
361 A_East is a diffuse clade occupying primarily coastal areas in Turkey. In the B_East clade, ten acces-
362 sions from central Anatolia form a well-supported group at the base of the clade. The rest of the

samples cover a large area from Baghdad to the Marmara Sea region and do not show an obvious mapping between phylogeny and geography.

Local and regional patterns of genetic diversity in Italy

The local and regional sampling in Italy allows us to take a closer look at how genetic diversity is distributed across small spatial scales. In Italy, the Apennines separate *B. distachyon* into genetically differentiated regional populations (Figure 5a). We here focus on four regional populations belonging to the A_Italia clade for which the largest number of samples is available (7-14). A TreeMix analysis with these populations suggests that no gene flow has occurred across the Appenines, as a tree-like model without migration edges explains 99.99% of the covariance of allele frequencies between populations (Figure S10).

Figure 5b shows pairwise genetic differences in the four populations, for which samples were collected few dozen meters to few kilometres apart. Within populations, some more closely related individuals stand out ($d_{XY} < 0.001$); these were typically collected within 1 km of each other. Most plants, however, even if growing close-by, are genetically quite distinct and can be more different from each other than from accessions kilometres away. Isolation by distance is weak at this scale and, while still significant in the two southern populations, is not significant in the Toscana and Emilia-Romagna populations. Genetic diversity declines step-wise from south to north, with a median d_{XY} of 0.0016 in Campania, 0.0015 in Abruzzo, 0.0014 in Toscana, and 0.0013 in Emilia-Romagna (Figure 5b).

Flowering phenology in the greenhouse and outdoors

Previous studies described the co-occurrence of the A_East and B_East clades in Turkey and interpreted the lack of gene flow between these lineages as a result of variation in flowering time: acces-

384 sions from the A_East clade require long vernalization and show a delay in flowering under greenhouse
385 conditions (Tyler et al., 2016; Gordon et al., 2017).

386 Our greenhouse experiment replicated the previously identified flowering behaviour of the
387 two B_East accessions Bd3-1 and BdTR3C and the two A_East accessions Bd1-1 and BdTR7a, which
388 in this order required four, six, eight, and more than 12 weeks to satisfy the vernalization response (Fig-
389 ure S11a, Table S2). With the exception of two C_Italia accessions which required six weeks of cold,
390 all other 10 newly tested Italian accessions required long periods (>10 weeks) of cold followed by up to
391 40 days in warm conditions to flower (Figure S11a, Table S2).

392 Flowering behaviour in the outdoor experiment was quite different (Figure S11b, Table S2).
393 All plants emerged in autumn and flowered next spring within two weeks. However, clades still differ
394 in their flowering behaviour. C_Italia and B_East accessions tended to produce flowers more rapidly
395 than A_East accessions, though this difference is not statistically significant at the 5% level. A_Italia
396 and B_West, on the other hand, take longer to flower than the other clades (LME, $P < 0.006$ for all com-
397 parisons between these two clades and the others), even though overall only two weeks separate the
398 early from late flowering accessions.

399 Discussion

400 *B. distachyon* was initially developed as a model to study gene function in grasses, with an emphasis on
401 applications in crop breeding. With this study we extend the genomic resources for this Mediterranean
402 grass and lay a foundation for evolutionary studies by providing a historical explanation for genetic
403 structure in the species. Population structure in *B. distachyon* is strongly hierarchical. It originated dur-
404 ing the Upper Pleistocene (c. 129,000 -11,700 years ago) and reflects, as we will argue in the following,

405 the combined effect of high selfing rates and effective seed dispersal. At the continental scale, dispersal
406 and selfing help to explain why highly diverged lineages might be present in the same locality without
407 signs of admixture. At the local scale, selfing and dispersal interact and maintain high local genetic di-
408 versity, with important implications for how natural selection is expected to act on the species.

409 Extreme selfing and extended heterozygosity as a result of recent outcrossing

410 In plants, the wide occurrence of sexual reproduction and the elaborate means evolved to ensure it sug-
411 gest that self-fertilization is disadvantageous under a wide range of conditions (Barrett, 2010). The best
412 known exception are colonizing plants (Baker, 1955; Stebbins, 1957): here, the advantage of reproduct-
413 ive assurance during colonization can outweigh the costs of inbreeding. *B. distachyon* clearly is a col-
414 onizing plant: it thrives in disturbed areas like pastures or along paths and declines when stable condi-
415 tions allow the establishment of perennial competitors (San Miguel, 2008).

416 Considering this life style, the highly reduced cleistogamous flowers (Khan & Stace, 1999;
417 Dinh Thi et al., 2016), and the general pattern that wind-pollinated species tend to be either predomin-
418 antly outcrossing or selfing (Barrett & Eckert, 1990), the highly selfing nature of *B. distachyon* comes
419 at no surprise. Nevertheless, the degree of homozygosity revealed by molecular markers is astonishing.
420 In a large-scale survey of 187 accessions from Turkey with 43 microsatellite markers, only four hetero-
421 zygous sites in four individuals were detected (Vogel et al., 2009). Similarly, Marques et al. (2017),
422 looking at 137 plants in 14 populations with 10 markers, estimated inbreeding coefficients of 1 in all
423 except one population.

424 Our study agrees with this finding and suggests that high selfing rates are prevalent throughout
425 the species' range. It also corrects previous estimates of heterozygosity based on genome-wide SNPs,
426 where we reported a median of 7.8 and 6.3% of heterozygous SNPs in the B_East and B_West clades

427 (Bourgeois et al., 2018). These estimates were most likely too high as we did not take into account arti-
428 ficial heterozygosity due to structural variation. Indeed, distinguishing real from artificial heterozygos-
429 ity proved to be challenging. As we show here, a method based on the clustering of heterozygous sites
430 and sequencing depth can be used to identify artificial heterozygosity arising from deletions and duplic-
431 ations. As plant population genomics is extending to more complex and dynamic genomes, searching
432 for islands of extended heterozygosity can be a simple first step to identify problems with heterozygous
433 sites and to limit biases in downstream analyses.

434 While self-fertilization appears to be the norm in *B. distachyon*, we also find evidence for re-
435 cent outcrossing. A large part of the heterozygosity we observed occurred in only six accessions, in the
436 form of extended islands of heterozygosity. Extended heterozygosity can result from the purging of de-
437 leterious homozygosity, as observed in inbred maize (Brandenburg et al., 2017), or from balancing se-
438 lection (Nordborg et al., 1996). These processes, however, imply a selective advantage of heterozygos-
439 ity and would hardly create hundreds of IEH in single accessions as observed here, but rather few IEH
440 present at higher frequencies. Our results thus provide evidence that the IEH in the six accession are
441 due to the admixture of diverged genotypes. As heterozygosity disappears within a few generations of
442 selfing (Hedrick, 2011), the outcrossing events leading to the six heterozygous accessions must be re-
443 cent and might have occurred during propagation of the accessions for research and seed distribution.

444 Shared ancestry reflects common descent rather than admixture

445 Historical gene flow can be inferred when the covariance of allele frequencies between populations is
446 poorly explained by tree-like evolution and genetic drift (Pickrell & Pritchard, 2012). Our tests for gene
447 flow between the five geographic clades and between regional populations in Italy suggest that patterns
448 of shared ancestry can largely be explained by tree-like descent rather than historical admixture. These

449 results contrast with previous studies which have interpreted shared ancestry as admixture (Gordon et
450 al., 2017; Stritt et al., 2018) and inferred frequent introgressions from incongruences between plastome
451 and nuclear phylogenies (Sancho et al., 2018). In the latter study, several B_East accessions are shown
452 to have B_West plastome genotypes, but no admixture is evident at the nuclear level, which the authors
453 explain through repeated backcrossing and loss of the B_West nuclear ancestry. Here too, however,
454 common descent and incomplete lineage sorting of plastome haplotypes are a plausible alternative ex-
455 planation, as for example described for *Hordeum* (Jakob & Blattner, 2006).

456 While outcrossing and historical gene flow remain a possibility, our results suggest that altern-
457 ative explanations for shared ancestry, more compatible with the extreme homozygosity and high self-
458 ing rates observed throughout *B. distachyon*, should be considered in future studies.

459 A scenario of separate migration corridors

460 To our current knowledge, *B. distachyon* in the Mediterranean region comprises three highly diverged
461 genetic lineages which can be further divided into geographic clades and regional populations. This ba-
462 sic tripartition was described previously in a genotyping-by-sequencing study (Tyler et al. 2016), yet a
463 biogeographic scenario to account for the distribution of the three lineages is now only starting to
464 emerge as samples from the entire species range are being collected (Skalska et al., 2020; Gordon et al.
465 2020). Here we show that the A lineage is present throughout Italy, and we describe a so far poorly
466 known lineage of *B. distachyon*, C_Italia.

467 The C lineage diverged from the others 86–128 kya and forms the basal branch in the phylo-
468 geny. Previous studies included single samples of this lineage, all originating from Sicily (Tyler et al.
469 2016, Gordon et al. 2020). We found this lineage to be present yet rare throughout Italy, in two in-
470 stances growing on the very same meadow as plants belonging to lineage A. Recently a similar situ-

471 ation has been described for *B. hybridum*, where individuals with a common ancestor more than one
472 million years ago coexist (Gordon et al., 2020; Shiposha et al., 2020). *Brachypodium* thus provides
473 striking examples of cryptic grass diversity in the Mediterranean region which would be difficult to ap-
474 preciate without the help of molecular markers.

475 The geographic co-occurrence of genetically diverged lineages in *B. distachyon* suggests that
476 three lineages of *B. distachyon* have expanded independently in the past, and that today, where their
477 ranges overlap, extreme selfing and possibly other reproductive barriers prevent interbreeding. While
478 the biogeography of the C lineage remains vague because of the low number of samples, an intriguing
479 scenario which could explain the disjunct genetic structure in *B. distachyon* is that lineages A and B
480 used different migration corridors: a North African corridor for lineage B, and a European corridor for
481 lineage A. To our knowledge, all samples collected in the Balkans so far belong to the A or the C lin-
482 eage (Tyler et al., 2016; Gordon et al., 2020; our unpublished data), suggesting that the B lineage is ab-
483 sent or rare between the Ligurian Alps and inland Turkey. With additional samples from the Balkans,
484 the Middle East, southern Spain and Africa, some of which have already been sequenced, this scenario
485 should be testable in the near future.

486 Our molecular dating analysis and the strong isolation by distance observed at the lineage
487 level suggest that the three lineage expansions in *B. distachyon* are not recent and might predate the end
488 of the Last Glacial Period c.11,700 years ago. The timescale we infer in this study, with a time to the
489 most recent common ancestor of 86 to 128 years ago, hinges on an assumed mutation rate of $7x10^{-9}$,
490 obtained from an experimental evolution study with *A. thaliana* (Ossowski et al., 2010). This estimate
491 is at the fast end of the spectrum as it reflects the accumulation of mutations before purifying selection
492 had a chance to remove them (Ho et al., 2011). Our estimates are therefore more likely too recent than

too old. A similar estimate, 162 ky to the common ancestor of the three lineages of *B. distachyon*, was recently obtained by time-calibrating an internal node rather than assuming a mutation rate (Gordon et al. 2020), providing further support for the timescale inferred here.

Genetic structure and flowering time differences

Previous studies have demoted geography to "a secondary factor in shaping population structure" (Gordon et al., 2017) and instead identified flowering time differences as "a main factor driving rapid intraspecific divergence" (Sancho et al., 2018; see also Tyler et al., 2016). This view is problematic as it is based on flowering phenotypes observed in the greenhouse. Flowering is a plastic trait and depends on environmental conditions (Gaudinier & Blackman 2020) and the timing of the other major life history event in annual plants, germination (Martínez-Berdeja et al., 2020). In our outdoors experiment, all accessions produced flowers within two weeks when they went through prolonged vernalization during winter. While this experiment does not reflect all the environmental variation present in *B. distachyon* natural habitats, it suggests that differences observed in the greenhouse might be exaggerated through artificially short vernalization times.

While the role of flowering in reproductive isolation is less clear than suggested by previous studies, flowering remains an intriguing trait in *B. distachyon*. A geographic pattern of flowering time differences is observed in Turkey but not in Italy. In Turkey, the A lineage, which requires vernalization to flower, is present along the coast, while the B lineage, which requires little to no vernalization (Gordon et al. 2017, Skalska et al. 2020, this study), is mainly found in inland Anatolia (Figure 2). Skalska et al. (2020) recently showed that the two lineages also differ in drought tolerance, indicating that the B_East accessions are adapted to the arid climate of central Anatolia. In Italy, no such geographic differences in vernalization requirement and flowering are observed, neither among lineages nor among

regional populations. Possibly this reflects the stronger ecological contrasts in Turkey, where rain is scarce on the inland Anatolian plateau even in winter, while the coastal regions have the typical Mediterranean winter rainfalls (Sensoy, 2008). Investigating the molecular evolution of flowering genes in *B. distachyon* will allow to further characterize the putative adaptive role of flowering time in this species.

Local consequences of selfing and dispersal

Within regional populations in Italy, isolation by distance is weak, and sampling within few hundred meters can yield individuals as different from each other as individuals kilometres apart (Figure 5). This pattern is discernible in the distribution of pairwise genetic differences and as long terminal branch lengths in the phylogeny, especially in the A lineage. Clearly the plants collected locally did not descend from single recent founder events, which would result in high local similarity. Our study thus supports the hypothesis that the interplay of high selfing and seed dispersal rates shapes local and regional genetic diversity, as proposed by Vogel et al. (2009) for populations in Turkey.

In population genetics textbooks, migration, gene flow, and interbreeding are often used synonymously (e.g. Charlesworth & Charlesworth, 2012), reflecting the dominance of animal models in the field. In plants, however, migration can occur through pollen and seed, and the migration of seeds need not imply the exchange of genetic material. With a selfing rate close to one, lineages can evolve independently of each other for a considerable period without the homogenizing effect of interbreeding, and lineage-specific mutations may accumulate. Seed dispersal would then ensure that closely related genotypes do not occur in patches, as observed in *A. thaliana* (Bomblies et al., 2010), but are shuffled across the landscape.

Central to the selfing-dispersal hypothesis is that *B. distachyon* disperses its seeds easily and over long distances. Morphological adaptations to do so have been described: the species has barbed palea which facilitates zoochory (Catalán et al., 2016). Surprisingly, however, so far no study mentioned the animals themselves, sheep and goats. From our fieldwork and previous reports (Vogel et al., 2009) it is clear that the habitat in which *B. distachyon* thrives are arid, oligotrophic pastures grazed by sheep and goats. Not only do these animals keep away more competitive perennial plants, but they are also known to carry plant seeds over long distances and to be an important vector of long-distance seed dispersal (Manzano & Malo, 2006). In the Mediterranean landscape, which has been shaped by human activity through thousands of years (Grove & Rackham, 2001), the movement of domestic animals might thus be a crucial factor in the population dynamics of *B. distachyon* and similar plants.

The possibility that genetic diversity is heavily influenced by long-distance seed dispersal has important implications for the study of natural selection in *B. distachyon.* While selfing itself decreases the fixation time of adaptive mutations and might favour local adaptation (Glémin & Ronfort, 2013; Hartfield et al., 2017), selfing combined with high rates of seed migration is expected to favour phenotypic plasticity over local adaptation (Sultan & Spencer, 2002). It is notable that no instance of a single lineage rising to high local frequencies is observed. Instead, it appears that seed dispersal maintains high local genetic diversity and might compensate for what is considered a main disadvantage of selfing: low diversity and failure to adapt to spatially and temporally heterogeneous environments (Wright et al., 2013).

Conclusion

What is a population of *B. distachyon*? *B. distachyon* is a generalist colonizing grass with large, continuous populations where pastoralism has not given way to intensive agriculture or forest (San Miguel,

2008; observations during fieldwork). As genotypes are shuffled across the landscape, a local sample is likely to capture the genotypic diversity of a broader region. Indeed, such a sample might include highly diverged genotypes coalescing only in the distant past, which might bias analyses relying on a purely spatial definition of "population". With these properties, *B. distachyon* is an interesting model to explore the limitations of classical population genetic models and to investigate the surprising ways in which the evolutionary play is acted out in nature.

Acknowledgments

The authors are especially thankful to the Swiss National Science Foundation and the University of Zurich's Research Priority Program (URPP) *Evolution in Action* for funding this project. AS, LAJM and RH acknowledge the funding from the National Science Centre Poland (grant no. 2015/18/M/NZ2/00394). The authors would like to thank the Genetic Diversity Center at ETH Zurich for providing access on their High Performance Computing resources as well as Christian Beisel at BSSE-Basel, Gerhard Herren and Helen Zbinden for their support in the lab. The authors also would like to thank Marco Maccaferri, Saverio Sciandrello and Pietro Minissale for their help in sampling in Italy, Jean-Paul Peltier for establishing connection between Switzerland and Morocco, Christian Parisod for his comments on an early draft of the manuscript and the three anonymous reviewers for contributing greatly to improving the manuscript.

References

Baker, H. G. (1955). Self-compatibility and establishment after “long-distance” dispersal. *Evolution*, *9*(3), 347–349. doi: 10.2307/2405656

Barrett, S. C. H. (2010). Darwin's legacy: the forms, function and sexual diversity of flowers. *Philosophical Transactions of the Royal Society B: Biological Sciences*, *365*(1539), 351–368. doi: 10.1098/rstb.2009.0212

Barrett, Spencer C H. (2003). Mating strategies in flowering plants: the outcrossing–selfing paradigm and beyond. *Philosophical Transactions of the Royal Society of London. Series B: Biological Sciences*, *358*(1434), 991–1004. doi: 10.1098/rstb.2003.1301

Barrett, Spencer C H, & Eckert, C. G. (1990). Variation and evolution of mating systems in seed plants. In S. Kawano (Ed.), *Biological Approaches and Evolutionary Trends in Plants* (pp. 229–254). London, UK: Academic Press.

Blasi, C., Capotorti, G., Copiz, R., Guida, D., Mollo, B., Smiraglia, D., & Zavattero, L. (2014). Classification and mapping of the ecoregions of Italy. *Plant Biosystems*, *148*(6), 1255–1345. doi: 10.1080/11263504.2014.985756

Bomblies, K., Yant, L., Laitinen, R. A., Kim, S. T., Hollister, J. D., Warthmann, N., … Weigel, D. (2010). Local-scale patterns of genetic variability, outcrossing, and spatial structure in natural stands of *Arabidopsis thaliana*. *PLoS Genetics*, *6*(3), 1–14. doi: 10.1371/journal.pgen.1000890

Bourgeois, Y., Stritt, C., Walser, J.-C., Gordon, S. P., Vogel, J. P., & Roulin, A. C. (2018). Genome-wide scans of selection highlight the impact of biotic and abiotic constraints in natural populations of the model grass *Brachypodium distachyon*. *The Plant Journal*, *96*(2), 438–451. doi: 10.1111/tpj.14042

Brandenburg, J. T., Mary-Huard, T., Rigaill, G., Hearne, S. J., Corti, H., Joets, J., … Tenaillon, M. I. (2017). Independent introductions and admixtures have contributed to adaptation of European maize and its American counterparts. *PLoS Genetics*, *13*(3), 1–30. doi: 10.1371/journal.pgen.1006666

Catalán, P., López-Álvarez, D., Bellosta, C., & Villar, L. (2016). Updated taxonomic descriptions, iconography, and habitat preferences of *Brachypodium distachyon*, *B. stacei*, and *B. hybridum* (Poaceae). *Anales del Jardin Botanico de Madrid*, *73*(1), 1–14. doi: 10.3989/ajbm.2428

Catalán, P., Müller, J., Hasterok, R., Jenkins, G., Mur, L. A. J. J., Langdon, T., … López-Alvarez, D. (2012). Evolution and taxonomic split of the model grass *Brachypodium distachyon*. *Annals of Botany*, *109*(2), 385–405. doi: 10.1093/aob/mcr294

Charlesworth, B, & Charlesworth, D. (2012). *Elements of Evolutionary Genetics*. Colorado, USA: Roberts and Company Publishers.

Charlesworth, Brian. (2009). Effective population size and patterns of molecular evolution and variation. *Nature Reviews Genetics*, *10*(3), 195–205. doi: 10.1038/nrg2526

Charlesworth, D. (2003). Effects of inbreeding on the genetic diversity of populations. *Philosophical Transactions of the Royal Society of London. Series B: Biological Sciences*, *358*(1434), 1051–1070. doi: 10.1098/rstb.2003.1296

Dell'Acqua, M., Zuccolo, A., Tuna, M., Gianfranceschi, L., & Pè, M. (2014). Targeting environmental adaptation in the monocot model *Brachypodium distachyon*: a multi-faceted approach. *BMC Genomics*, *15*(1), 801. doi: 10.1186/1471-2164-15-801

Dray, S., & Dufour, A.-B. B. (2007). The ade4 package: Implementing the duality diagram for ecologists. *Journal of Statistical Software*, *22*(4), 1–20. doi: 10.18637/jss.v022.i04

Engelmann, K., & Purugganan, M. (2006). The molecular evolutionary ecology of plant development: flowering time in *Arabidopsis thaliana*. *Advances in Botanical Research*, *44*(06), 507–526. doi: 10.1016/S0065-2296(06)44013-1

Evanno, G., Regnaut, S., & Goudet, J. (2005). Detecting the number of clusters of individuals using the software STRUCTURE: A simulation study. *Molecular Ecology*, *14*(8), 2611–2620. doi: 10.1111/j.1365-294X.2005.02553.x

Flouri, T., Jiao, X., Rannala, B., & Yang, Z. (2018). Species tree inference with BPP using genomic sequences and the multispecies coalescent. *Molecular Biology and Evolution*, *35*(10), 2585–2593. doi: 10.1093/molbev/msy147

Frichot, E., & François, O. (2015). LEA: An R package for landscape and ecological association studies. *Methods in Ecology and Evolution*, *6*(8), 925–929. doi: 10.1111/2041-210X.12382

Gaudinier, A., & Blackman, B. K. (2020). Evolutionary processes from the perspective of flowering time diversity. *New Phytologist*, *225*(5), 1883–1898. doi: 10.1111/nph.16205

Gibson, D. J. (2009). *Grasses & Grassland Ecology*. Oxford University Press.

Giraldo, P., Rodríguez-Quijano, M., Vázquez, J. F., Carrillo, J. M., & Benavente, E. (2012). Validation of microsatellite markers for cytotype discrimination in the model grass *Brachypodium distachyon*. *Genome*, *55*(7), 523–527. doi: 10.1139/g2012-039

Glémin, S., & Ronfort, J. (2013). Adaptation and maladaptation in selfing and outcrossing species: New mutations versus standing variation. *Evolution*, *67*(1), 225–240. doi: 10.1111/j.1558-5646.2012.01778.x

Gordon, S. P., Contreras-Moreira, B., Levy, J. J., Djamei, A., Czedik-Eysenberg, A., Tartaglio, V. S., … Vogel, J. P. (2020). Gradual polyploid genome evolution revealed by pan-genomic analysis of *Brachypodium hybridum* and its diploid progenitors. *Nature Communications*, *11*(1), 1–16. doi: 10.1038/s41467-020-17302-5

Gordon, S. P., Contreras-Moreira, B., Woods, D. P., Des Marais, D. L., Burgess, D., Shu, S., … Vogel, J. P. (2017). Extensive gene content variation in the *Brachypodium distachyon* pan-genome correlates with population structure. *Nature Communications*, *8*(1). doi: 10.1038/s41467-017-02292-8

Griffin, P. C., & Willi, Y. (2014). Evolutionary shifts to self-fertilisation restricted to geographic range margins in North American *Arabidopsis lyrata*. *Ecology Letters*, *17*(4), 484–490. doi: 10.1111/ele.12248

Grove, A., & Rackham, O. (2001). *The Nature of Mediterranean Europe - An Ecological History*. Yale University Press.

Hadfield, J. D. (2010). MCMC methods for multi-response generalized linear mixed models: The MCMCglmm R package. *Journal of Statistical Software*, *33*(2), 1–22. doi: 10.18637/jss.v033.i02

Hartfield, M., Bataillon, T., & Glémin, S. (2017). The evolutionary interplay between adaptation and self-fertilization. *Trends in Genetics*, *33*(6), 420–431. doi: 10.1016/j.tig.2017.04.002

Hartfield, M., Wright, S. I., & Agrawal, A. F. (2018). Coalescence and linkage disequilibrium in facultatively sexual diploids. *Genetics*, *210*(2), 683–701. doi: 10.1534/genetics.118.301244

Hedrick, P. (2011). *Genetics of Populations*. Jones & Bartlett Publishers.

Hey, J., & Machado, C. A. (2003). The study of structured populations–new hope for a difficult and divided science. *Nature Reviews Genetics*, *4*(7), 535–543. doi: 10.1038/nrg1112

Ho, S. Y. W. W., Lanfear, R., Bromham, L., Phillips, M. J., Soubrier, J., Rodrigo, A. G., & Cooper, A. (2011). Time-dependent rates of molecular evolution. *Molecular Ecology*, *20*(15), 3087–3101. doi: 10.1111/j.1365-294X.2011.05178.x

Huo, N., Garvin, D. F., You, F. M., McMahon, S., Luo, M. C., Gu, Y. Q., … Vogel, J. P. (2011). Comparison of a high-density genetic linkage map to genome features in the model grass *Brachypodium distachyon*. *Theoretical and Applied Genetics*, *123*(3), 455–464. doi: 10.1007/s00122-011-1598-4

International Brachypodium Initiative (2010). Genome sequencing and analysis of the model grass *Brachypodium distachyon*. *Nature*, *463*(7282), 763–768. doi: 10.1038/nature08747

Jakob, S. S., & Blattner, F. R. (2006). A chloroplast genealogy of Hordeum (Poaceae): Long-term persisting haplotypes, incomplete lineage sorting, regional extinction, and the consequences for phylogenetic inference. *Molecular Biology and Evolution*, *23*(8), 1602–1612. doi: 10.1093/molbev/msl018

Khan, M. A., & Stace, C. a. (1999). Breeding relationships in the genus *Brachypodium* (Poaceae: Pooideae). *Nordic Journal of Botany*, *19*(3), 257–269. doi: 10.1111/j.1756-1051.1999.tb01108.x

Lawson, D. J., Hellenthal, G., Myers, S., & Falush, D. (2012). Inference of population structure using dense haplotype data. *PLoS Genetics*, *8*(1), 11–17. doi: 10.1371/journal.pgen.1002453

Lee, T.-H., Guo, H., Wang, X., Kim, C., & Paterson, A. H. (2014). SNPhylo: a pipeline to construct a phylogenetic tree from huge SNP data. *BMC Genomics*, *15*(1), 162. doi: 10.1186/1471-2164-15-162

Li, H. (2013). Aligning sequence reads, clone sequences and assembly contigs with BWA-MEM. *ArXiv*. doi: 10.1093/bioinformatics/btw748

Li, R., Li, Y., Fang, X., Yang, H., Wang, J., Kristiansen, K., & Wang, J. (2009). SNP detection for massively parallel whole-genome resequencing. *Genome Research*, *19*(6), 1124–1132. doi: 10.1101/gr.088013.108

Linhart, Y. B., & Grant, M. C. (1996). Evolutionary significance of local genetic differentiation in plants. *Annual Review of Ecology and Systematics*, *27*(1), 237–277. doi: 10.1146/annurev.ecolsys.27.1.237

López-Alvarez, D., Manzaneda, A. J., Rey, P. J., Giraldo, P., Benavente, E., Allainguillaume, J., … Catalan, P. (2015). Environmental niche variation and evolutionary diversification of the Brachypodium distachyon grass complex species in their native circum-Mediterranean range. *American Journal of Botany*, *102*(7), 1073–1088. doi: 10.3732/ajb.1500128

López-Alvarez, Diana, López-Herranz, M. L., Betekhtin, A., & Catalán, P. (2012). A DNA barcoding method to discriminate between the model plant *Brachypodium distachyon* and its close relatives *B. stacei* and *B. hybridum* (Poaceae). *PLoS ONE*, *7*(12), e51058. doi: 10.1371/journal.pone.0051058

Loveless, M. D., & Hamrick, J. L. (1984). Ecological determinants of genetic structure in plant populations. *Annual Review of Ecology and Systematics. Vol. 15*, *15*(May), 65–95. doi: 10.1146/annurev.es.15.110184.000433

Manzano, P., & Malo, J. E. (2006). Extreme long-distance seed dispersal via sheep. *Frontiers in Ecology and the Environment*, *4*(5), 244–248. doi: 10.1890/1540-9295(2006)004[0244:ELSDVS]2.0.CO;2

Marques, I., Shiposha, V., L?pez-Alvarez, D., Manzaneda, A. J., Hernandez, P., Olonova, M., & Catalán, P. (2017). Environmental isolation explains Iberian genetic diversity in the highly homozygous model grass *Brachypodium distachyon*. *BMC Evolutionary Biology*, *17*(1), 139. doi: 10.1186/s12862-017-0996-x

Martínez-Berdeja, A., Stitzer, M. C., Taylor, M. A., Okada, M., Ezcurra, E., Runcie, D. E., & Schmitt, J. (2020). Functional variants of DOG1 control seed chilling responses and variation in seasonal life-history strategies in *Arabidopsis thaliana*. *Proceedings of the National Academy of Sciences of the United States of America*, *117*(5), 2526–2534. doi: 10.1073/pnas.1912451117

Morgulis, A., Gertz, E. M., Schäffer, A. A., & Agarwala, R. (2006). A fast and symmetric DUST implementation to mask low-complexity DNA sequences. *Journal of Computational Biology*, *13*(5), 1028–1040. doi: 10.1089/cmb.2006.13.1028

Nieto Feliner, G. (2014). Patterns and processes in plant phylogeography in the Mediterranean Basin. A review. *Perspectives in Plant Ecology, Evolution and Systematics*, *16*(5), 265–278. doi: 10.1016/j.ppees.2014.07.002

Nordborg, M., Charlesworth, B., & Charlesworth, D. (1996). Increased levels of polymorphism surrounding selectively maintained sites in highly selfing species. *Proceedings of the Royal Society B: Biological Sciences*, *263*(1373), 1033–1039. doi: 10.1098/rspb.1996.0152

Nordborg, Magnus. (2000). Linkage disequilibrium, gene trees and selfing: An ancestral recombination graph with partial self-fertilization. *Genetics*, *154*(2), 923–929.

Ossowski, S., Schneeberger, K., Lucas-Lledó, J. I., Warthmann, N., Clark, R. M., Shaw, R. G., … Lynch, M. (2010). The rate and molecular spectrum of spontaneous mutations in *Arabidopsis thaliana*. *Science*, *327*(5961), 92–94. doi: 10.1126/science.1180677

Pannell, J. R., & Fields, P. D. (2014). Evolution in subdivided plant populations: Concepts, recent advances and future directions. *New Phytologist*, *201*(2), 417–432. doi: 10.1111/nph.12495

Pebesma, E. J., & Bivand, R. S. (2005). Classes and methods for spatial data in R. *R News*, *5*(2), 9–13. Retrieved from http://cran.r-project.org/doc/Rnews/

Pickrell, J. K., & Pritchard, J. K. (2012). Inference of population splits and mixtures from genome-wide allele frequency data. *PLoS Genetics*, *8*(11). doi: 10.1371/journal.pgen.1002967

Platt, A., Horton, M., Huang, Y. S., Li, Y., Anastasio, A. E., Mulyati, N. W., … Borevitz, J. O. (2010). The scale of population structure in *Arabidopsis thaliana*. *PLoS Genetics*, *6*(2), e1000843. doi: 10.1371/journal.pgen.1000843

Putman, A. I., & Carbone, I. (2014). Challenges in analysis and interpretation of microsatellite data for population genetic studies. *Ecology and Evolution*, *4*(22), 4399–4428. doi: 10.1002/ece3.1305

Quinlan, A. R., & Hall, I. M. (2010). BEDTools: A flexible suite of utilities for comparing genomic features. *Bioinformatics*, *26*(6), 841–842. doi: 10.1093/bioinformatics/btq033

Rambaut, A., Drummond, A. J., Xie, D., Baele, G., & Suchard, M. A. (2018). Posterior summarization in Bayesian phylogenetics using Tracer 1.7. *Systematic Biology*, *67*(5), 901–904. doi: 10.1093/sysbio/syy032

Rannala, B., & Yang, Z. (2003). Bayes estimation of species divergence times and ancestral population sizes using DNA sequences from multiple loci. *Genetics*, *1656*(August), 1645–1656.

Ream, T. S., Woods, D. P., Schwartz, C. J., Sanabria, C. P., Mahoy, J. A., Walters, E. M., … Amasino, R. M. (2014). Interaction of photoperiod and vernalization determines flowering time of *Brachypodium distachyon*. *Plant Physiology*, *164*(2), 694–709. doi: 10.1104/pp.113.232678

San Miguel, A. (2008). Management of Natura 2000 habitats. 6220: Pseudo-steppe with grasses and annuals of the Thero-Brachypodietea. *European Commission.*

Sancho, R., Cantalapiedra, C. P., López-Alvarez, D., Gordon, S. P., Vogel, J. P., Catalán, P., & Contreras-Moreira, B. (2018). Comparative plastome genomics and phylogenomics of *Brachypodium*: flowering time signatures, introgression and recombination in recently diverged ecotypes. *New Phytologist*, *218*(4), 1631–1644. doi: 10.1111/nph.14926

Scholthof, K. B. G., Irigoyen, S., Catalan, P., & Mandadi, K. K. (2018). *Brachypodium*: A monocot grass model genus for plant biology. *Plant Cell*, *30*(8), 1673–1694. doi: 10.1105/tpc.18.00083

Sensoy, S. (2008). *Climate of Turkey*. Turkish State Meteorological Service.

Sharma, N., Ruelens, P., D'Hauw, M., Maggen, T., Dochy, N., Torfs, S., … Geuten, K. (2017). A flowering locus C homolog is a vernalization-regulated repressor in *Brachypodium* and is cold regulated in wheat. *Plant Physiology*, *173*(2), 1301–1315. doi: 10.1104/pp.16.01161

Shiposha, V., Marques, I., López-Alvarez, D., Manzaneda, A. J., Hernandez, P., Olonova, M., & Catalán, P. (2020). Multiple founder events explain the genetic diversity and structure of the model allopolyploid grass *Brachypodium hybridum* in the Iberian Peninsula hotspot. *Annals of Botany*, *125*(4), 625–638. doi: 10.1093/aob/mcz169

Skalska, A., Stritt, C., Wyler, M., Williams, H. W., Vickers, M., Han, J., … Mur, L. A. J. (2020). Genetic and methylome variation in Turkish *Brachypodium distachyon* accessions differentiate two geographically distinct subpopulations. *International Journal of Molecular Sciences*, *21*(18), 1–17. doi: 10.3390/ijms21186700

Stebbins, G. L. (1957). Self fertilization and population variability in the higher plants. *The American Naturalist*, *91*(861), 337–354. doi: 10.1086/281999

Stein, N., Herren, G., & Keller, B. (2001). A new DNA extraction method for high-throughput marker analysis in a large-genome species such as *Triticum aestivum*. *Plant Breeding*, *120*(4), 354–356. doi: 10.1046/j.1439-0523.2001.00615.x

Stritt, C., Gordon, S. P., Wicker, T., Vogel, J. P., & Roulin, A. C. (2018). Recent activity in expanding populations and purifying selection have shaped transposable element landscapes across natural accessions of the Mediterranean grass *Brachypodium distachyon*. *Genome Biology and Evolution*, *10*(1), 304–318. doi: 10.1093/gbe/evx276

Stritt, C., Wyler, M., Gimmi, E. L., Pippel, M., & Roulin, A. C. (2020). Diversity, dynamics and effects of long terminal repeat retrotransposons in the model grass *Brachypodium distachyon*. *New Phytologist*, *227*(6), 1736–1748. doi: 10.1111/nph.16308

Sultan, S. E., & Spencer, H. G. (2002). Metapopulation structure favors plasticity over local adaptation. *The American Naturalist*, *160*(2), 271–283. doi: 10.1086/341015

Tarasov, A., Vilella, A. J., Cuppen, E., Nijman, I. J., & Prins, P. (2015). Sambamba: Fast processing of NGS alignment formats. *Bioinformatics*, *31*(12), 2032–2034. doi: 10.1093/bioinformatics/btv098

Thi, V. H. D., Coriton, O., Le Clainche, I., Arnaud, D., Gordon, S. P., Linc, G., … Chalhoub, B. (2016). Recreating stable *Brachypodium hybridum* allotetraploids by uniting the divergent genomes of *B. distachyon* and *B. stacei*. *PLoS ONE*, *11*(12), 1–27. doi: 10.1371/journal.pone.0167171

Thompson, J. D. (2005). *Plant Evolution in the Mediterranean*. Oxford University Press.

Tyler, A. L., Lee, S. J., Young, N. D., Deiulio, G. A., Benavente, E., Reagon, M., … Caicedo, A. L. (2016). Population structure in the model grass *Brachypodium distachyon* is highly correlated with flowering differences across broad geographic areas. *The Plant Genome*, 1–55. doi: 10.3835/plantgenome2015.08.0074

Vogel, J. P. (2016). Genetics and Genomics of Brachypodium. Springer International Publishing.

Vogel, J. P., Tuna, M., Budak, H., Huo, N., Gu, Y. Q., & Steinwand, M. a. (2009). Development of SSR markers and analysis of diversity in Turkish populations of *Brachypodium distachyon*. *BMC Plant Biology*, *9*, 88. doi: 10.1186/1471-2229-9-88

Waples, R. S., & Gaggiotti, O. (2006). What is a population? An empirical evaluation of some genetic methods for identifying the number of gene pools and their degree of connectivity. *Molecular Ecology*, *15*(6), 1419–1439. doi: 10.1111/j.1365-294X.2006.02890.x

Wright, S. (1931). Evolution in Mendelian populations. *Genetics*, *16*(97). doi: 10.4161/hv.21408

Wright, S. I., Kalisz, S., & Slotte, T. (2013). Evolutionary consequences of self-fertilization in plants. *Proceedings. Biological Sciences / The Royal Society*, *280*(1760), 20130133. doi: 10.1098/rspb.2013.0133

Zhang, C., Dong, S. S., Xu, J. Y., He, W. M., & Yang, T. L. (2019). PopLDdecay: A fast and effective tool for linkage disequilibrium decay analysis based on variant call format files. *Bioinformatics*, *35*(10), 1786–1788. doi: 10.1093/bioinformatics/bty875

Zheng, X., Levine, D., Shen, J., Gogarten, S. M., Laurie, C., & Weir, B. S. (2012). A high-performance computing toolset for relatedness and principal component analysis of SNP data. *Bioinformatics*, *28*(24), 3326–3328. doi: 10.1093/bioinformatics/bts606

Data Accessibility

Illumina paired-end sequencing data generated for this project are available on the European Nucleotide Archive, project number PRJEB40344.

Author Contributions

ACR, LAJM, RH obtained funding for the project. ACR and CS designed the study. ACR, AHB, CS, NP and RH collected samples. CS analysed the data, with input and help from ACR, AS, ELG and MW. CS wrote the original draft, and all authors reviewed it.

Figures

Figure 1

Islands of extended heterozygosity (IEH) among hard-filtered SNPs (x axis) and among SNPs in high confidence regions (y axis), defined as regions where at least 90 percent of the accessions have a read coverage within 1.5 standard deviations of their mean coverage. (a) Overview of all 196 accessions, highlighting the six outlier accessions. (b) Zoom-in on the red square in panel a.

Figure 2

Geographic origin and genetic structure. (a) Map and pie charts showing shared ancestry. Only a subset of accessions is displayed for the dense local samples in Italy and France. (b) Cross-entropy for increasing K in the ancestry analysis with sNMF. (c) Rooted phylogeny with divergence times, estimated under a multispecies coalescent model. (d) Principal component analysis. (e) Rooted phylogeny and coancestry matrix estimated with fineSTRUCTURE, as well as sNMF barplot for K=5. The fineSTRUCTURE chunk length is the recombination map distance donated to individuals in rows from individuals in columns (log scale). Names in italics highlight regional populations, asterisks indicate small clusters: * Accessions from northern Italy, including a cluster of five accessions from Taro valley in Emilia-Romagna. ** ABR9 collected in Albania and three accessions from the Gargano peninsula. ***

Arn1 and Mon3. **** Three Turkish accessions clustering with Bd30-1 from southern Spain. ***** Accessions from Sicily, Campania and Liguria. An interactive phylogenetic tree/map can be explored on github.com/cstritt/bdis-phylogeo.

Figure 3

Decay of linkage disequilibrium at different scales of population structure: (a) species-wide, (b) in the three major genetic lineages, (c) in four geographic clades (C_Italia is not included as it is the sole representative of lineage C and thus already included at the lineage level), (d) four regional populations in Italy.

Figure 4

Genetic diversity and differentiation. (a) Pairwise genetic differences (d_{XY}) within and between the five geographic clades. One panel is shown for each clade, the colours within the panel showing with which clade pairwise comparisons are made. (b) Correlation between geographic and genetic distance within the three major genetic lineages A, B and C. Colours within the panels indicate between which geographic regions pairwise comparisons are made. Correlation coefficients from Mantel test and their significance are displayed.

Figure 5

Genetic differentiation across ecoregions in Italy. (a) Map showing the ecoregion classification of Blasi et al. (2014) and *B. distachyon* habitats in the four sampled regional populations. (b) Genetic diversity within the A_Italia clade, for which the most extensive sampling is available. Boxplots show the distribution of d_{XY} across the whole clade and within regional populations, while dotplots show how d_{XY} relates to geographic distance.

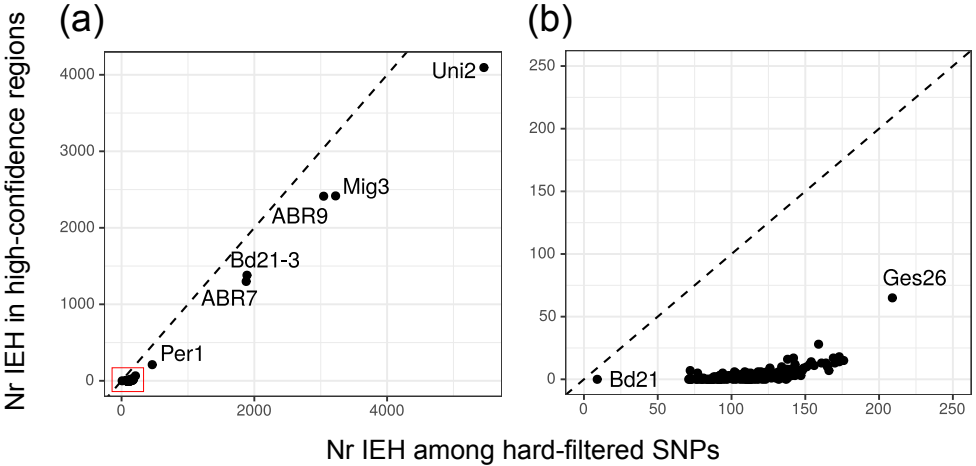
(a)
(b)
Nr IEH in high-confidence regions
Nr IEH among hard-filtered SNPs
Uni2
Mig3
ABR9
Bd21-3
ABR7
Per1
Ges26
Bd21
0
1000
2000
3000
4000
0
50
100
150
200
250

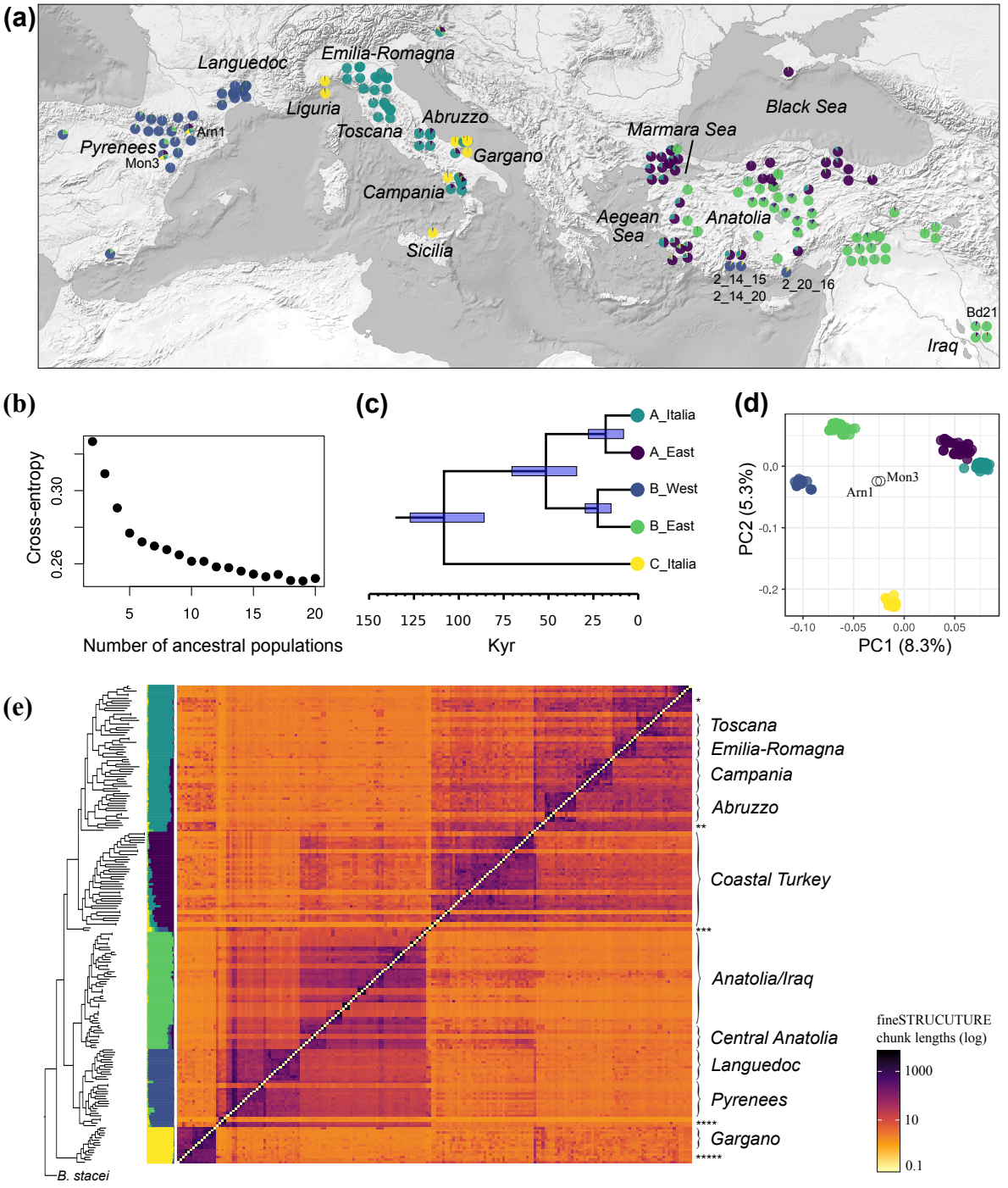
(a)
Languedoc
Emilia-Romagna
Liguria
Toscana
Abruzzo
Gargano
Campania
Sicilia
Pyrenees
Arn1
Mon3
Black Sea
Marmara Sea
Aegean Sea
Anatolia
2_14_15
2_14_20
2_20_16
Bd21
Iraq
(b)
Cross-entropy
0.30
0.26
5
10
15
20
Number of ancestral populations
(c)
A_Italia
A_East
B_West
B_East
C_Italia
150
125
100
75
50
25
0
Kyr
(d)
PC2 (5.3%)
0.0
-0.1
-0.2
Mon3
Arn1
-0.10
-0.05
0.00
0.05
PC1 (8.3%)
(e)
Toscana
Emilia-Romagna
Campania
Abruzzo
Coastal Turkey
Anatolia/Iraq
Central Anatolia
Languedoc
Pyrenees
Gargano
B. stacei
fineSTRUCUTURE
chunk lengths (log)
1000
10
0.1

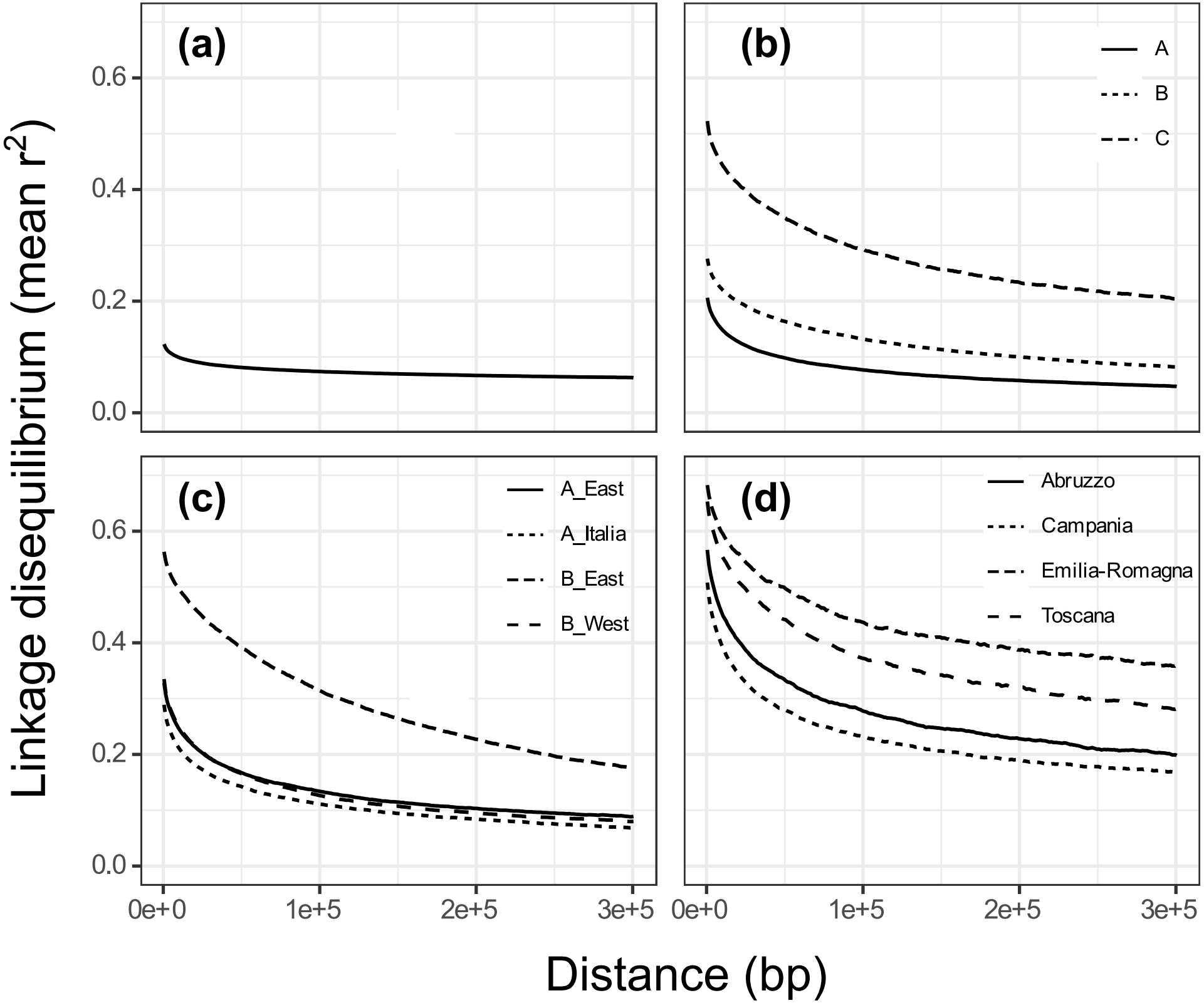
(a)
(b)
(c)
(d)
A
B
C
A_East
A_Italia
B_East
B_West
Abruzzo
Campania
Emilia-Romagna
Toscana
0.0
0.2
0.4
0.6
0e+0
1e+5
2e+5
3e+5
Linkage disequilibrium (mean r2)
Distance (bp)

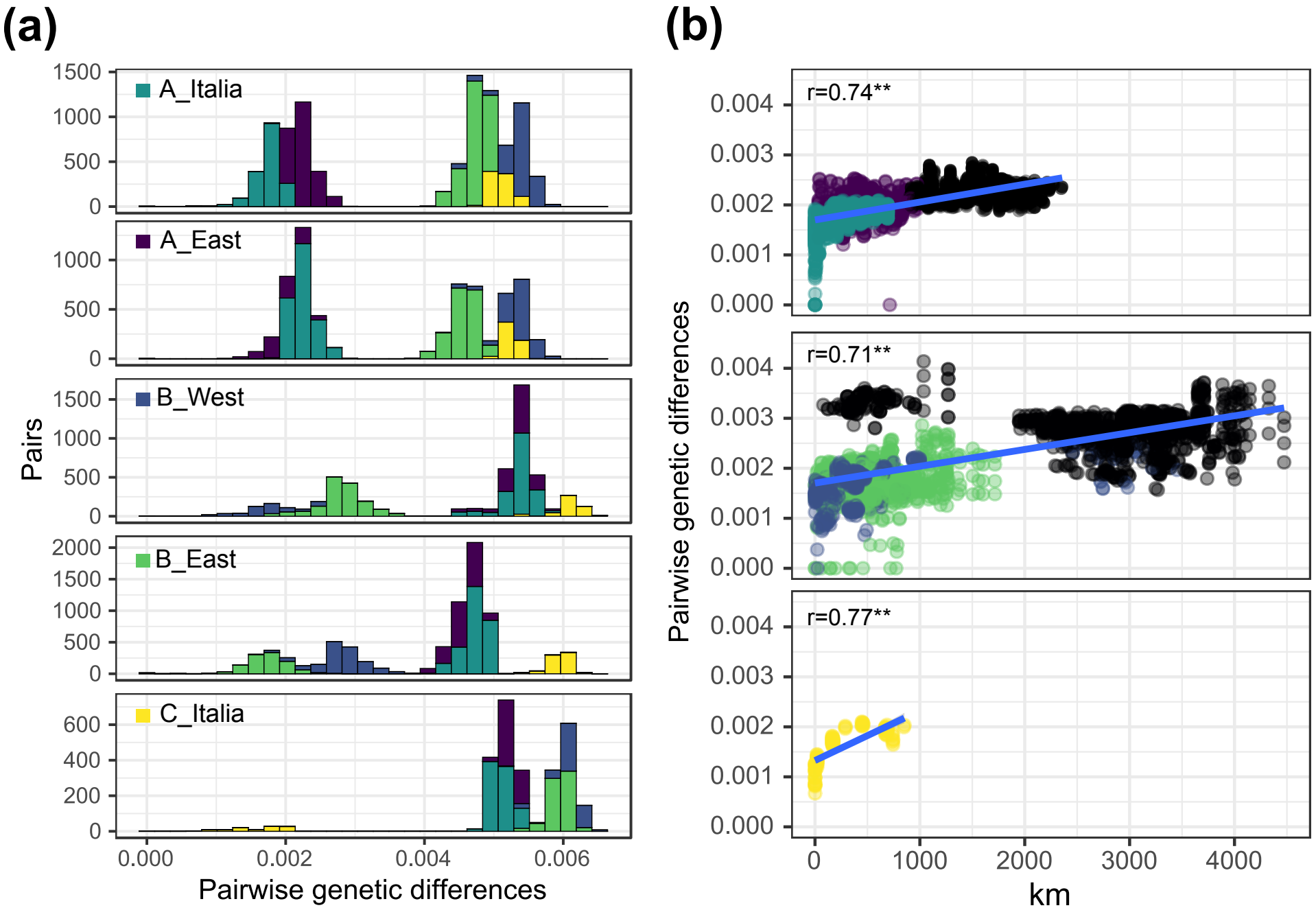
(a)
A_Italia
A_East
B_West
B_East
C_Italia
Pairs
Pairwise genetic differences
(b)
r=0.74**
r=0.71**
r=0.77**
Pairwise genetic differences
km

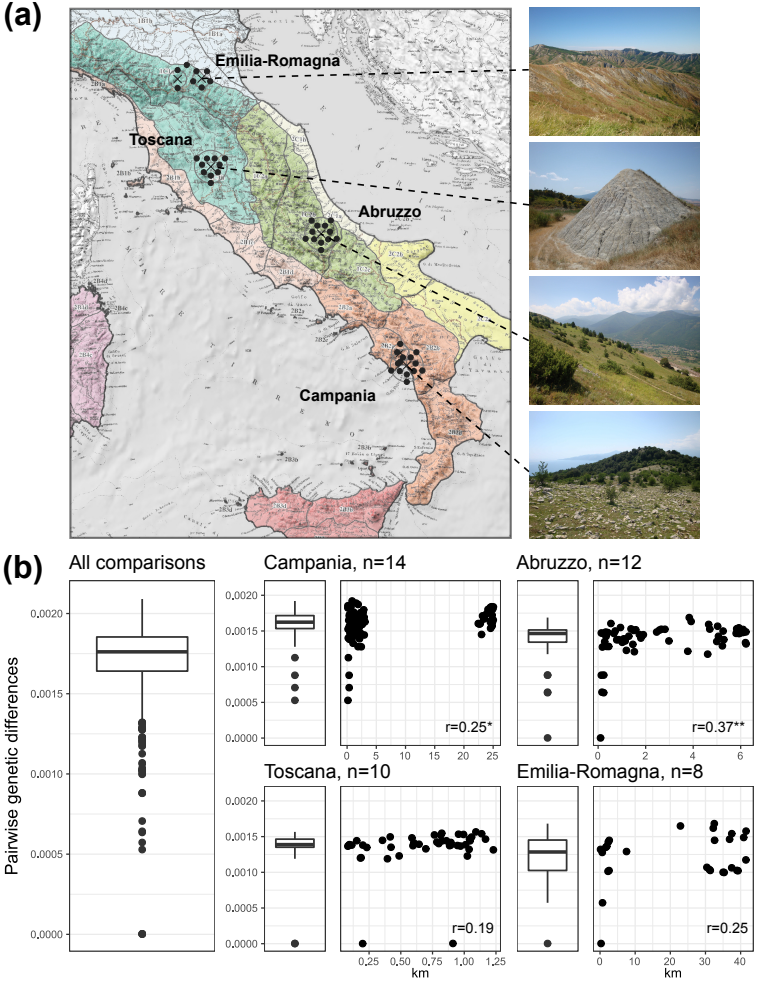
(a)
Emilia-Romagna
Toscana
Abruzzo
Campania
(b)
All comparisons
Campania, n=14
Abruzzo, n=12
Toscana, n=10
Emilia-Romagna, n=8
Pairwise genetic differences
r=0.25*
r=0.37**
r=0.19
r=0.25
km
km